Beilstein-Institut
Functional Nanoscience
May 17th – 21st, 2010, Bozen, Italy

Energy Transductions in ATP Synthase

Christoph von Ballmoos, Alexander Wiedenmann and Peter Dimroth*

Institute of Microbiology, Swiss Federal Institute of Technology (ETH) Zürich, Wolfgang-Pauli-Straße 10, 8093 Zürich, Switzerland

E-Mail: *dimroth@micro.biol.ethz.ch

Received: 30th August 2010 / Published: 13th June 2011

Abstract

Life depends on chemical energy in the form of adenosinetriphosphate (ATP), most of which is produced by the F_1F_o ATP synthase, a rotary nanomachine. Here, we report new insights into the torque-generating mechanism by the membrane-embedded F_o motor. High coupling ion concentrations on the ion entrance side are required to prepare the motor for rotation. In the absence of this condition, the motor is in a resting state, where the stator arginine is assumed to form a complex with the conserved carboxyl group of an empty rotor site. At high coupling ion concentrations, however, the motor switches into a mobile state, in which an incoming coupling ion has displaced the arginine and has formed a new complex with the rotor site. At appropriate driving forces, the ion dissociates from the next incoming rotor site and escapes into the cytoplasmic reservoir of the membrane. The resulting negatively charged site is attracted by the positively charged arginine, which elicits rotation and generates torque.

Introduction

Life is dependent on a continuous input of energy. Light or nutrients serve as external energy source which is converted into the cell intrinsic energy currency ATP. In order to do so, photosynthetic reaction centres in specific membranes of green plants or phototrophic bacteria harvest the light to transfer electrons and protons across the membrane and thereby generate an electro-chemical proton gradient. Animals and heterotrophic bacteria use energy

from the combustion of nutrients for proton translocation by respiratory enzymes to generate an electrical potential across the membrane, while certain anaerobic bacteria dispose of membrane-bound Na^+-translocating decarboxylases to carry out this task [1]. The free energy thus stored in the charged membranes is used by the universal F_1F_o ATP synthase to combine ADP and phosphate to ATP, thereby conserving the energy in its terminal pyrophosphate bond (Figure 1). Upon hydrolysis of this bond, the stored energy is released and can be used to drive numerous energy-consuming cellular reactions, *e.g.* biosynthesis of many cellular compounds, ion transport, motility, signal transduction, etc.. Hence, continuous cycling between ATP synthesis and hydrolysis is a prerequisite to fulfil the cell's energy needs. The dimension of this cell energy cycle is astounding, amounting to a daily turnover of 50 kg ATP in a human on average.

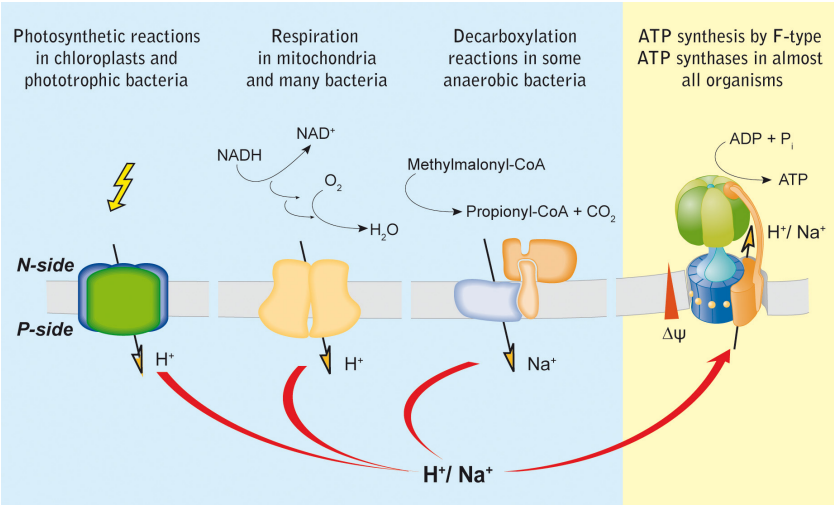

Figure 1. Ion cycling across biological membranes leading to ATP synthesis (modified from [5]). Chloroplasts and phototrophic bacteria convert light energy into an electrochemical proton gradient across the membrane. In heterotrophic organisms like animals or bacteria the metabolism of nutrients generates reducing equivalents (NADH, succinate) that are reoxidized by the respiratory chain enzymes using oxygen as terminal electron acceptor. The free energy is converted into an electrochemical gradient of protons across the membrane. The anaerobic bacterium *P. modestum* couples the decarboxylation of methylmalonyl-CoA to electrogenic Na^+-transport. The electrochemical H^+ or Na^+ gradients established by these membrane-bound complexes serve as energy source for ATP synthesis from ADP and inorganic phosphate by an F_1F_o ATP synthase.

The ATP synthase is a miniature machine composed of two rotary motors, F_1 and F_o, which are mechanically connected to assure energy exchange amongst them [2 – 5]. The F_1 motor is a water soluble protein complex which displays the following subunit composition α_3, β_3, γ. δ, ε. The F_o motor is membrane-embedded and exists in its simplest form as subunits a, b_2, and $c_{10\text{-}15}$ (Figure 2). In the ATP synthesis mode, the F_o motor converts the electro-

chemical gradient of H^+ or Na^+ ions into torque, enabling the F_1 motor to act as an ATP generator. In the ATP hydrolysis mode, F_1 converts the chemical energy of ATP hydrolysis into torque, causing the membrane-embedded F_o motor to act as an ion pump. Generally, the F_o motor generates the larger torque and forces the F_1 motor to function in ATP synthesis direction. In most eukaryotes and some bacteria, the hydrolysis mode is tightly regulated or blocked to avoid unnecessary energy waste. However, in fermenting bacteria, when the respiratory enzymes are not active, the F_1 motor hydrolyses ATP to employ the F_o motor to generate the membrane potential which is indispensable for every living cell.

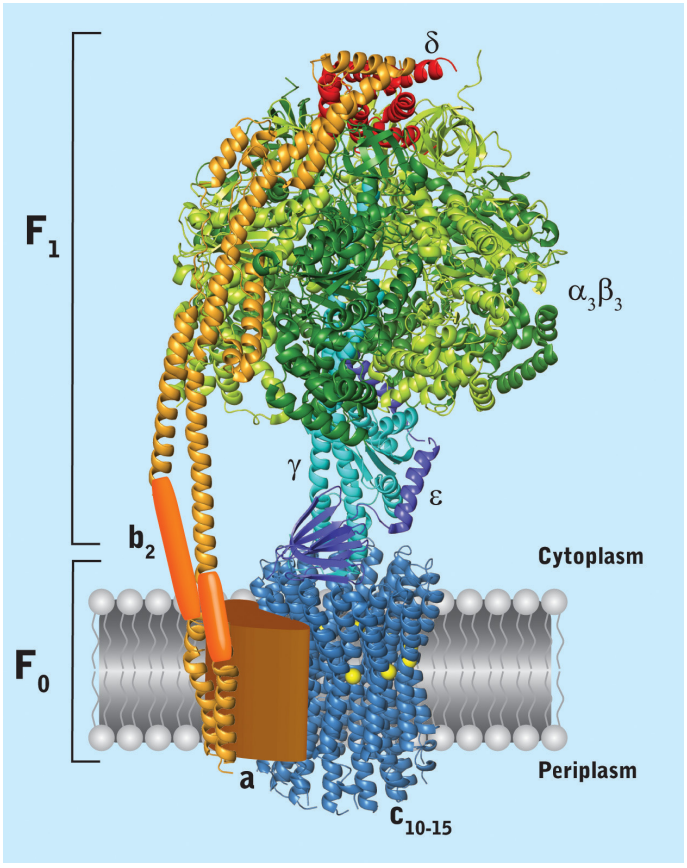

Figure 2. Organization of a bacterial F_1F_o ATP synthase (modified from [5]). The structures of individual sub-complexes were taken from RCSB Protein Data Base and assembled by eye according to biochemical data. The structures used were from the c ring of *I. tartaricus* (1CYE), the F_1 organization of *E. coli* (1JNV), the δ subunit of *E. coli* (2A7U), the peripheral stalk from bovine mitochondria (2CLY) and the membranous part of subunit b of *E. coli* (1B9U). No high resolution structural data are available for subunit a and the hinge region of subunit b. The picture was created using Pymol (DeLano Scientific LLC).

The crystal structure of F_1 from bovine heart mitochondria revealed a hexameric assembly of alternating α and β subunits around an eccentric α-helical coiled-coil γ subunit [6]. The catalytic centre consists of three nucleotide binding sites on the β subunits at the interface with the α subunits. At any one time each of these sites is in a different conformation and performs a different task in the synthesis or hydrolysis of ATP. The actual conformation of a site depends on its specific interaction with the γ subunit which changes upon rotation of γ in a coordinated sequence. Each site thus cycles through the same set of open and closed conformations with the corresponding functions in the uptake, processing and release of nucleotides [7].

Kinetic details of the binding change mechanism have been revealed from single molecule studies with isolated F_1 molecules. Thereby, the γ subunit was observed to rotate in discrete steps of 120° for each ATP molecule hydrolyzed [8]. Under limiting ATP concentrations, the 120° rotation can be divided into 80° and 40° sub-step rotations, associated with ATP binding and ATP hydrolysis followed by product release, respectively [9, 10]. Single molecule experiments were also performed with the intact F_1F_o ATP synthase reconstituted in lipid vesicles [11, 12]. Here, compiled by the subunits γ, ε and the c_{10-15} ring the rotor turns counter clockwise in the ATP hydrolysis direction and clockwise in the ATP synthesis direction, when viewed from the F_o domain. When proteoliposomes prepared with F_1F_o from *Escherichia coli* were properly energized for ATP synthesis, the rotor turned with a stepping size of 36°, reflecting a stepping motion for each individual c subunit in the oligomeric c_{10} ring [13].

The F_o Motor

The rotary F_o motor of the ATP synthase obtains its driving force from an electrochemical ion gradient across the membrane. The only other ion-driven rotary motors in nature are the A_o portion of archaeal A_1A_o ATPases, the V_o portion of vacuolar V_1V_o ATPases and the flagellar motor. While A_o and V_o are phylogenetically related to F_o, the flagellar motor is much larger and has a different construction. The central element of the F_o motor is an oligomeric ring of 10 – 15 copies of c subunits. Each c subunit consists of two membrane-spanning α-helices that are connected by a hydrophilic loop on the cytoplasmic side of the membrane. In the c ring, the loop regions form an extensive area of contact, where the ring combines with the foot of the central stalk subunits γ and ε to form the rotor assembly [14, 15]. At the periphery of the c ring, the F_o motor consists of subunits a and b_2. Subunit a is a very hydrophobic protein containing 5 or 6 membrane-spanning α-helices, which actively participates in the ion translocation mechanism [16, 17]. The b subunits are anchored within the membrane by an N-terminal α-helix and extend as the peripheral stalk all the way to the head of the F_1 domain [18 – 20]. Near their N-terminus, the b subunits contact the C-terminal part of the c subunits and the periplasmic loop of subunit a between helices 4 and 5. With their C-terminal ends, the b subunits form a strong complex with the δ and the α subunit and thus serve to connect the stator parts of F_o (a, b_2) with those of F_1 (α_3, β_3, δ). This

connection is an important device to counter the tendency of the stator to follow the rotation of the rotor. The X-ray structure of the mitochondrial peripheral stalk indicates that it is rather rigid and therefore well suited for its anticipated function [21].

Structure of c Rings and their Binding Sites

Na^+ binding sites

For a functional understanding of the F_o motor, structural knowledge is essential. Hence, the high resolution structure of the c ring from the Na^+-translocating ATP synthase of *Ilyobacter tartaricus* was an important step towards this goal. In the X-ray structure at 2.8 Å resolution [22], the oligomeric ring with 11 subunits appears as an hourglass-shaped hollow cylinder (Figure 2). The centre of the cylinder encloses a hydrophobic cavity which is filled with phospholipids in the natural environment of the membrane [23]. Each c monomer folds into a helical hairpin with the loop at the cytoplasmic side and the termini at the periplasmic side of the membrane. The N-terminal helices form a tightly packed inner ring with no space for large side chains which is accounted for by a conserved motif of four glycine residues [24]. In addition, the tight packing of the glycines causes the inner ring of helices to narrow from the cytoplasm toward the middle of the membrane. The 11 C-terminal helices of the outer ring pack into the grooves of the inner ring in the cytoplasmic half of the protein. All helices show a bend of about 20° in the middle of the membrane (at P28 and E65 in the N-terminal and C-terminal helices, respectively), marking the narrowest part of the hourglass shape. Eleven Na^+ ions are located here at their binding sites, facing toward the outer surface of the c ring, which is consistent with cross-linking data [25].

With respect to the function, the most important insights derive from the structure of the ion binding site. Each of the 11 Na^+ ions is bound at the interface of one N-terminal and two C-terminal helices. The coordination sphere is formed by the side-chain oxygens of Q32 and E65 of one subunit and of the side chain oxygen of S66 plus the carbonyl oxygen of V63 of the neighbouring subunit. A fifth Na^+ coordination site is provided by the oxygen of a structural water molecule, which is held in place by donating hydrogen bonds to the carbonyl oxygen of A64 and the side chain oxygen of T67 [26] (Figure 3a). The structure of the ion binding site is remarkably similar to that of the larger k-ring from the V-ATPase of *Enterococcus hirae* [27]. In this structure, all five Na^+ coordination sites are directly contributed from the protein and structural water is not involved. The coordination sphere is completed by a network of hydrogen bonds. The side chain oxygen of E65 which is involved in Na^+ coordination also receives a hydrogen bond from the NH_2 group of Q32, and the other oxygen of E65 receives hydrogen bonds from the OH groups of S66 and Y70. These hydrogen bonds serve to keep E65 deprotonated at physiological pH in order to allow Na^+ binding. The mutation Y70F, *e.g.*, prohibits hydrogen bonding of Y70 with E65 and leads to a 30-fold decreased affinity for Na^+ [31]. The wild type arrangement, however, creates a stable, locked conformation, from which horizontal transfer of the Na^+ ion to

subunit a is prevented. In the subunit a/c interface, the conformation of the binding site must therefore convert to an open one, to allow ion transfer between the binding site and subunit a (see below).

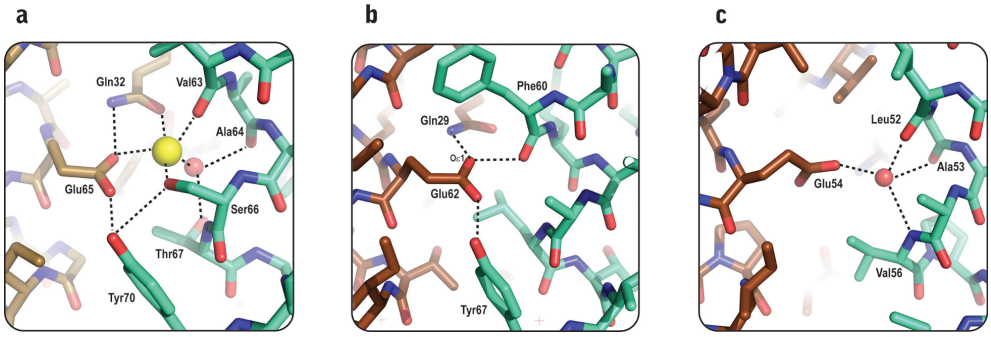

Figure 3. View on the three types of ion binding sites in F-type ATP synthases. (a) Na^++H_2O ion binding site in the c_{11}-ring of *I. tartaricus* (2wgm). **(b)** H^+-binding site in the c_{15}-ring of *S. platensis* (2wie). **(c)** H^++H_2O-binding in the c_{13}-ring of *B. pseudofirmus* OF4 (2 × 2v). Every binding site is made up from residues of two neighbouring subunits (brown and cyan). Amino acids involved in ion binding site coordination are indicated. The hydrogen bonding network is indicated by dashed lines. The Na^+ ion (yellow) and the water molecules (red) are shown as spheres. In **(b)** The oxygen atom on Glu62 harbouring the H^+ is highlighted with $O_{\varepsilon 1}$.

Two different ion binding modes can be envisaged for the proton-translocating ATP synthases. Either, the binding site involves several ligands to form a coordination sphere for ion binding in analogy to that of the Na^+-translocating ATP synthases. In this case, the proton would be bound to water and the resulting hydronium ion would be coordinated. Alternatively, the entire binding site could consist of just the conserved carboxylate allowing protons to hop on and off in a group protonation type mechanism, as proposed in most F_o motor models. The structure of the c_{15} ring from the H^+-translocating ATP synthase from the cyanobacterium *Spirulina platensis* [28] shows that its overall shape resembles that of the c ring from *I. tartaricus*. Intriguingly, the conformation of the conserved glutamate that is essential for ion binding is stabilized by a hydrogen bonding network which is similar to that of the Na^+ binding c-rings. As the authors point out, the conserved glutamate must be protonated in the crystallization buffer at pH 4.3 and indeed, one oxygen atom ($O_{\varepsilon 1}$) of this glutamate appears to act as a hydrogen bond donor for the backbone carbonyl oxygen of F60 from the neighbouring subunit (Figure 3b). Hence, the pH 4.3 structure is in accordance to the group protonated carboxylate that is expected at this acidic pH. However, it does not provide any clues on whether the binding site glutamate remains in its group protonated form at physiological pH values or participates in the coordination of a hydronium ion. To discriminate between these options, the structure must be determined at neutral pH.

Very recently, the c-ring structure of the alkaliphilic bacterium bacillus OF4 has been determined from crystals grown at pH 4.3 and a water molecule is clearly visible in the ion binding pocket (Figure 3c) [29]. Furthermore, the F1-c10 structure from yeast suggests the coordination of water because H-bonding as described above for the *S. platensis* c-ring is not possible [30]. Interestingly, the yeast structure has been determined from crystals grown at pH 7.5. Although it cannot be clarified from the existing binding site structures, if the coupling proton is indeed coordinated as a hydronium ion, the presence of structured water renders old models of simple protonation/deprotonation of the ion binding carboxylates highly unlikely.

Besides this structural work, the mode of proton binding has been investigated by biochemical techniques [31]. The well known modification of the binding site carboxylate with the inhibitor *N,N'*-dicyclohexylcarbodiimide (DCCD) consumes a proton and can therefore be used to monitor the proton availability at the binding site. The pH profile for DCCD labelling of the ATP synthase from *Halobacterium salinarium* or *I. tartaricus* in its H^+-translocation mode (in the absence of Na^+) showed a typical titration curve with maximum labelling rates at pH 6 and below, half maximal labelling rates around pH 7, and no detectable labelling at pH 8 and above. Hence, these enzymes show the expected behaviour for a group protonation of the binding site carboxylate.

For the majority of the H^+-ATP synthases, including enzymes from *E. coli*, spinach chloroplasts and bovine mitochondria, however, bell-shaped labelling pH profiles were observed with maximum labelling rates between pH 7.5 and 9 and decreasing rates at lower or higher pH values. These data are clearly not compatible with a simple group protonation of the binding site. They would be consistent, however, with hydronium ion binding in the physiological (neutral) pH range and a shift to group protonation at acidic pH, when the proton concentration approaches the dissociation constant of the binding site carboxylate. The decreasing labelling rates at acidic pH values may be related to the robust conformation of the binding site seen in the group-protonated structure of the *S. platensis* c ring at pH 4.3 [28]. This may have an inferior reactivity for substitution by DCCD compared to the conformation with a bound hydronium ion in the physiological near neutral pH range. Higher labelling rates at pH 7 than at pH 5.5 or 10 were also observed with the *S. platensis* c ring, but whether this can be attributed to structural differences of the binding pocket at the different pH values has not yet been rationalized [32].

These results not only provide evidence for distinct proton binding modes in the ATP synthase family but also show that the degree of binding site protonation depends on the external pH. As DCCD reacts with binding sites outside the subunit a/c interface, this implies that there is an access pathway for the protons to the binding sites in the absence of subunit a [33, 34]. Whether this access route is sufficiently fast to meet physiological conditions is presently unknown. Multiple lines of evidence indicate that the ions reach the sites from the cytoplasmic reservoir of the membrane. Interestingly, the pH profiles for

DCCD labelling of the various ATP synthases were remarkably similar to those of the ATP hydrolysis activities of the F_1F_o holoenzymes [31]. We anticipate that the rate limiting step in the ATP hydrolysis mode of the enzyme is the loading of the binding site in the subunit a/c interface from the cytoplasmic side of the membrane, because electrostatic constraints prevent the rotation of an unoccupied site with its negative charge into the hydrophobic membrane environment [35]. Hence, the rate of ATP hydrolysis is dependent on the cytoplasmic pH value and on the dissociation constant of the binding site at the cytoplasmic access route in the subunit a/c interface. Similar dissociation constants for the site at this location and outside the interface with subunit a may be the rationale for the similarity of the DCCD labelling and ATP hydrolysis pH profiles.

The Role of Subunit a

Structural information on subunit a is sadly very limited, but important details of its function have nevertheless been uncovered in the past decades. There is general agreement that the a subunit contributes the physiological access routes from the periplasm and the cytoplasm to the binding sites and that the conserved arginine is located in between these routes, blocking unhindered proton flux. In elaborative studies with cysteine mutants of subunit a from *E. coli*, the ion accessible parts have been probed [36, 37]. These data suggest that an ion accessible channel, located in the centre of helices $2-5$ of subunit a, extends from the periplasm to the centre of the membrane. The cytoplasmic access route to the binding site, however, remained ambiguous, because only few residues near the cytoplasmic surface of the fourth transmembrane helix of the a subunit were accessible. Recently, the cytoplasmic half of the outer helices of subunit c were also found to contain ion accessible sites, which therefore suggests that the cytoplasmic access pathway is located in the interface between subunit a and c [38]. Such an access route would be consistent with cysteine/cysteine cross linking data with the *E. coli* and *I. tartaricus* ATP synthase, which show that helix IV of the a subunit is in close proximity to the outer helices of the c ring [39, 40]. Recent cryo-electron microscopy data on the structure of the V-ATPase of *Thermus thermophilus*, however, indicate only a small area of contact between the stator and the c ring equivalent near the centre of the membrane [41].

The most important residue of subunit a is the membrane-embedded, conserved arginine (position 210 in *E. coli*), also known as the stator charge. So far, every mutation of this residue in the *E. coli* enzyme led to a complete loss of activity [42], whereas in the Na^+-translocating *P. modestum* enzyme, mutations retaining the positive charge were tolerated under specific conditions [43]. In the ATP hydrolysis mode, the stator charge is believed to ensure dissociation of the coupling ion from a c ring site entering the interface with the a subunit. Accordingly, ATP hydrolysis became uncoupled from Na^+ translocation by mutagenesis of the stator arginine to alanine in the *P. modestum* ATP synthase. A second function of the arginine is to provide a seal between the two access pathways to prevent ion leakage

across the membrane [44]. In the ATP synthesis mode, the role of the arginine is probably more sophisticated, since it not only affects the ion binding affinity of the site at the periplasmic channel, but also plays a profound role in the generation of torque (see below).

Insights into the mode of interaction of the stator arginine with the ion binding site have been obtained by cysteine-cysteine cross-linking experiments between subunits a and c of the *I. tartaricus* ATP synthase [40]. From the available c ring structure with its locked binding site conformation, one could predict a conformational change in the interface with subunit a to facilitate ion transfer between the c ring site and the a subunit. Strong evidence for a small but significant conformational change upon contact with the stator charge derives from the cross-linking patterns between cT67C or cG68C and aN230C. Whereas in the locked conformation, the two c ring residues from neighbouring subunits occupy spatially similar positions toward a potent binding partner on subunit a, only cT67C, but not cG68C, could form efficient cross-links with aN230C in the presence of the stator charge. Upon mutagenesis of the stator arginine by uncharged amino acids, the cross-linking efficiency of aN230C with cT67C remained unchanged, but that with cG68C increased significantly. From this and other data, the stator charge is proposed to induce a conformational change in the empty binding site, by which cG68C is disconnected from its cross-linking partner in subunit a. Relating these observations to the c ring structure suggests a rearrangement of the binding site residues with the side chain of cE65 being slightly pushed or rotated toward the c ring centre, thereby affecting the accessibility of cG68C (which is on the same helix) but not of cT67C (which is on the neighbouring helix). The spatial demand for this rearrangement is presumably allocated by a cavity between the inner and the outer ring of helices in the region of the two conserved residues G25 and G68 (Figure 4a). Accordingly, replacement of G25 by a bulky isoleucine increased the cross-linking efficiency of the cG68C/aN230C pair to a similar extent as the replacement of the stator charge. No ATP synthesis was observed with the cG25I mutant, emphasizing the functional importance of the small residue. The interpretations were supported by energy minimization calculations of the c ring structure with a short strip of helix 4 of subunit a, containing residues aI225 to aM231, which suggested possible modes for the interaction of the arginine with an unoccupied binding site (Figure 4b).

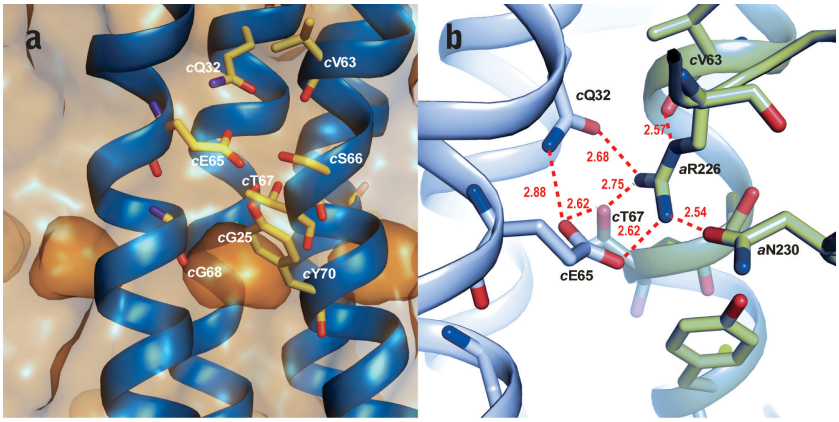

Figure 4. Interaction of the a subunit with the c-ring (modified from [40]). (a) Perspective view on the surface of the isolated c-ring of *I. tartaricus*. Shown are the atom boundaries displayed as surface to visualize the cavity below the ion binding site. Further, the residues of the ion binding site and the glycine residues cG25 and cG68 around the cavity are depicted (see text for details). **(b)** Coordination of the stator arginine after energy minimization calculations of the c-ring and a heptapeptide of helix 4 of subunit a. Depicted are the calculated positions and possible hydrogen bonds of the binding site residues on the c-ring and the stator arginine in the absence of harmonic backbone restraints of the outer helices. Putative hydrogen bond lengths are marked in Å. The figure was prepared using Pymol (DeLano Scientific).

Driving Forces for ATP Synthesis

An electrochemical gradient of either H^+ or Na^+ provides the driving force for ATP synthesis by F_1F_o ATP synthases. The downhill movement of these ions through the F_o domain generates torque which is transmitted to F_1 to energize ATP synthesis. The driving force consists of two thermodynamically equivalent parameters, the ion concentration gradient (ΔpH or ΔpNa^+) and the membrane potential ($\Delta\psi$). Most organisms use the proton motive force ($\Delta\mu H^+$) with the parameters ΔpH and $\Delta\psi$, but some anaerobic bacteria use the sodium motive force consisting of ΔpNa^+ and $\Delta\psi$ for the synthesis of ATP.

Proton motive force driven ATP synthesis was originally formulated in Mitchell's chemiosmotic model, which also implies that ΔpH and $\Delta\psi$ are equivalent kinetic driving forces [45]. Early experiments with the chloroplast enzyme seemed to support this notion, because ATP synthesis could be driven by ΔpH alone [46]. The method to establish the ΔpH by an acid/base transition with succinate as the acidic buffer, however, was later shown to also create a significant $\Delta\psi$, owing to the membrane permeability of the succinate monoanion [47]. An equivalent of ΔpH and $\Delta\psi$ as driving forces for ATP synthesis has also been described for the mitochondrial enzyme [48, 49]. Accordingly, it was predicted that ATP synthesis occurs when the thermodynamic requirements are fulfilled, i.e. if

$$\Delta\mu H^+ = \Delta\psi + \Delta pH > \Delta Gp = \Delta G^{o\prime} x \log_{10} [ATP]/([ADP] x [P_i]).$$

Several investigations involving a variety of ATP synthases have subsequently shown that the equivalence of ΔpH and Δψ as driving force for ATP synthesis is not perfect [50 – 52], suggesting that different kinetic barriers have to be overcome by either ΔpH or Δψ. In all these studies, except for the chloroplast enzyme from spinach, efficient ATP synthesis required a total driving force of > 180 mV, consisting of a minimal Δψ of ~80 mV and a corresponding ΔpH.

Requirements for ATP Synthesis

ATP synthesis measurements have been performed with a number of ATP synthases, but the most complete data are available for the H^+-translocating ATP synthase of *E. coli* or spinach chloroplasts and the Na^+-translocating ATP synthases of *P. modestum* or *I. tartaricus,* respectively. With *E. coli* membrane vesicles energized by respiration, a turnover number for ATP synthesis of about 270 s^{-1} was found [53]. For the reconstituted *E. coli* enzyme, the maximal rates of ATP synthesis were 80 s^{-1}, when the vesicles were energized with a total driving force of 380 mV, consisting of a ΔpH of 240 mV and a Δψ of 140 mV [52]. In this study, the rate decreased drastically to ~1 s^{-1} if the ΔpH of 240 mV was maintained and the Δψ was abolished. These results confirm the notion that ATP synthesis requires both parameters of the proton motive force and that these are kinetically not equivalent.

In the same study, ATP synthesis was also abolished by decreasing the ΔpH to ~180 mV at Δψ values between 110 and 150 mV. This is remarkable, because the energetic parameters ($\Delta\mu H^+ = 290 - 330$ mV) clearly exceeded those found in a growing *E. coli* cell. The discrepancy could be resolved in more recent studies with the reconstituted *E. coli* enzyme, where it was observed that the rate of ATP synthesis not only depends on the driving forces ΔpH and Δψ, but also on the proton concentration on the source (P) side of the membrane [54]. In these experiments, efficient ATP synthesis was found at significantly lower driving forces (ΔpH = 120 mV; Δψ = 120 mV) than in the previous studies, if the P-side pH values were kept below 6. The rate decreased sharply at higher pH values and reached undetectable levels at pH 7 and above (Figure 5a). Effective ATP synthesis therefore not only depends on an appropriate size of the two driving forces ΔpH and Δψ, but also on a sufficiently high proton concentration at the P-side. From a physiological point of view, this result causes a dilemma, because *E. coli* cells grow perfectly well and synthesize ATP at pH values of 8 and above. Lateral proton transfer along the membrane surface between the respiratory chain enzymes and the ATP synthase might be an elegant solution to generate sufficiently high proton concentrations at the entrance port of the ATP synthase to make ATP synthesis feasible [55]. In contrast, the requirements of the Na^+-driven ATP synthase of *P. modestum* are nicely met by its natural environment of brackish water (50 – 150 mM NaCl).

The high proton concentration requirement is not observed during ATP hydrolysis, where the fully coupled enzyme operates at nearly maximal speed at pH > 8.5. Hence, approximately 100-times higher proton concentrations are necessary to saturate the binding sites at

the periplasmic entrance channel during ATP synthesis than at the cytoplasmic entrance channel during ATP hydrolysis. Studies with the ATP synthase of spinach chloroplast are in agreement with the notion above except that the enzyme is capable of synthesizing ATP in the presence of a large ΔpH only [52].

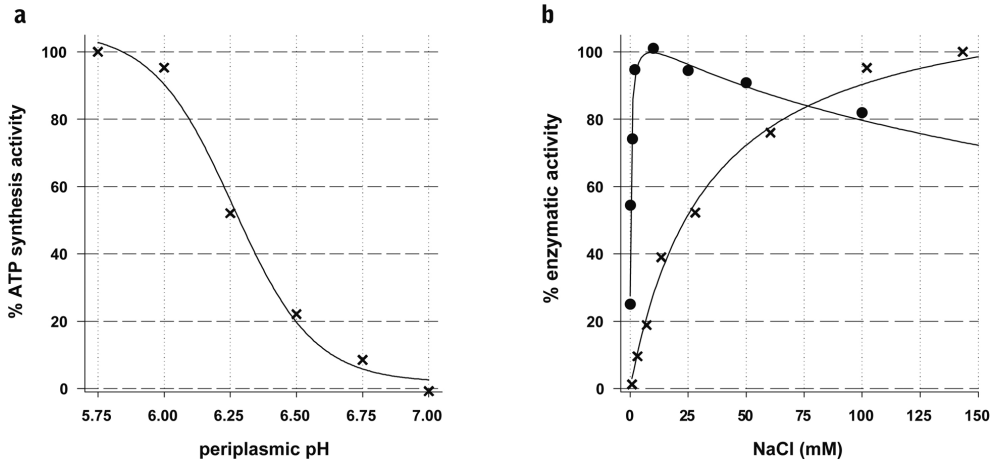

Figure 5. Importance of the coupling ion concentration on the *P*-side during ATP synthesis. **(a)** ATP synthesis with purified ATP synthase of *E. coli* reconstituted in proteoliposomes. At constant driving forces of $\Delta\psi = 120$ mV and $\Delta pH = 2$ (122 mV), half maximal ATP synthesis is observed at a P-side pH 6.2. No ATP synthesis is observed at pH values above 7. **(b)** ATP synthesis with purified ATP synthase of *P. modestum* reconstituted in proteoliposomes. At constant driving forces of $\Delta\psi = 140$ mV and $\Delta pNa = 120$ mV, half maximal ATP synthesis is observed at a P-side Na^+ concentration of ~35 mM (crosses). In contrary, half maximal ATP hydrolysis is already observed at a Na^+ concentration of ~0.5 mM (closed circles).

Corresponding observations have also been made with the Na^+-translocating ATP synthase of *P. modestum*. ATP synthesis required both parameters of the sodium motive force with a minimum ΔpNa^+ of > 30 mV and a minimum $\Delta\psi$ of > 180 mV and in addition P side Na^+ concentrations of ~35 mM for half maximal activities [54]. This Na^+ concentration requirement for ATP synthesis was approximately 70 – 100 times higher than that for half maximal ATP hydrolysis [56, 57] (Figure 5b). Hence, in spite of the different coupling ions, the ATP synthases of *E. coli* and *P. modestum* exhibit a remarkable similar asymmetry in their coupling ion concentration requirements for ATP synthesis or hydrolysis. A reasonable explanation for this asymmetry most likely reflects different affinities of the binding sites for the coupling ion at the periplasmic and cytoplasmic access routes of subunit a. The affinity of the binding site will be affected at each specific location by the chemical environment of the a subunit, particularly the interaction with the stator charge.

Implications for the F_o Motor Function

In a current model of the F_o motor, the arginine is assumed to form a complex with the negatively charged empty binding site between the periplasmic and cytoplasmic access channels of subunit a [54]. Ion binding to an arginine-bound site is expected to require higher ion concentrations than ion binding to a free site. In the ATP hydrolysis mode of the enzyme, the torque applied from the F_1 motor is likely to disrupt the arginine-binding site complex with the result that the affinity of the site at the cytoplasmic channel is no longer affected by the stator charge. Very similar affinities for the binding sites outside the interface with subunit a and at the cytoplasmic entrance route during ATP hydrolysis support this view (see above). In the ATP synthesis mode of the enzyme, however, the complex of the binding site with the arginine must first be broken before the site can form the new complex with the incoming coupling ion and therefore, higher coupling ion concentrations are required to compete successfully with the stator charge to occupy the sites at the periplasmic entrance channel.

It is important that sufficiently high P-side coupling ion concentrations are an essential requirement for the synthesis of ATP, which cannot be compensated by very high $\Delta pH/\Delta pNa^+$ and/or $\Delta\psi$ values. This suggests that the events creating rotation must follow a given sequence, which starts with the replacement of the arginine by an incoming coupling ion at the periplasmic channel. Ion dissociation from the following binding site at the cytoplasmic channel is in equilibrium with the ion concentration at the cytoplasmic side and is probably favoured by the positive charge of the arginine and the membrane potential (see below). After dissociation, the new negatively charged site is immediately attracted by the positively charged arginine, causing rotation and the generation of torque and resulting in a new arginine/binding site complex.

Importantly, the membrane potential did not affect the ion binding affinity of the site of the periplasmic channel of the Na^+-ATP synthase [54]. This implies that the potential has no influence on the initial replacement of the arginine from the binding site by Na^+ entering from the periplasmic side. The potential therefore probably exerts its effect on the events at the cytoplasmic channel. This is consistent with the more hydrophobic nature of this channel compared to the periplasmic one, as observed in accessibility studies [36].

The mechanism of the F_o motor has also been investigated by ion translocation experiments through the isolated F_o part. While most of these studies did not take the orientation of F_o within the membrane into account, it is now clear that detailed insights require transport measurements in each specific direction with unidirectionally reconstituted F_o complexes [58]. Proton transport measurements were performed with the reconstituted F_o complexes of *E. coli* in both directions. With a constant driving force of $\Delta\psi = 73$ mV or $\Delta pH = 73$ mV the rate of proton transport was about $600\ s^{-1}$ in synthesis direction and about $1400\ s^{-1}$ in hydrolysis direction. Hence, in one specific direction, similar rates were produced by each

driving force, which are therefore equivalent for the F_o part. The transport rates corresponded linearly to the applied driving forces and no voltage threshold was apparent. The most significant difference between H^+ transport in synthesis and hydrolysis direction was observed, when the influence of the pH was determined. Proton transport in hydrolysis direction remained almost constant over the entire pH range from 6.5 to 9, thus resembling the ATP hydrolysis pH profile. In contrast, proton transport through F_o in synthesis direction decreased continuously with increasing P-side pH values from 6 to 9, with half maximal velocity at pH 7.7 and less than 20% of the initial rate at pH 9. Thus, the pH profile for H^+ transport in synthesis direction resembles the ATP synthesis pH profile, except for a shift of the apparent pK_a from 7.7 to 6.2. This shift may be related to the demand of increased torque during ATP synthesis, where counteracting conformational restraints in the F_1 part have to be overcome. These restraints exposed by the F_1 part may also be responsible for the necessity of a minimum membrane potential of ~60 mV for ATP synthesis, but not for H^+ conduction through the isolated F_o complex.

Na^+ transport through F_o of the *P. modestum* ATP synthase has also been measured in both directions [54, 59]. In synthesis direction, Na^+ transport could be driven either by ΔpNa^+ or by $\Delta\psi$ and maximal rates were obtained, if the two driving forces were applied simultaneously. ATP synthesis and Na^+ transport through F_o in the appropriate direction thus responded to the same driving forces, except for the more stringent conditions for ATP synthesis, which required both driving forces simultaneously, whereas only one was sufficient for the ion conduction. In contrast, Na^+ transport through F_o in ATP hydrolysis direction was entirely dependent on $\Delta\psi$ and did not respond to the applied ΔpNa^+. Relating these results to the F_o motor model described above, they suggest that the arginine/binding site complex can only interact with ions entering from the periplasmic but not from the cytoplasmic side of the membrane. The arginine is therefore replaced from the complex with the binding site by high periplasmic but not by high cytoplasmic Na^+ concentrations. To break the complex from the cytoplasmic side obviously requires the membrane potential, which corroborates the notion that the potential interacts with the F_o motor through its cytoplasmic access route.

A New Model for the F_o Motor

In conclusion, these results suggest a novel mechanism for the F_o motor operation. In the resting state, an empty binding site near the periplasmic access channel of subunit a forms a complex with the stator arginine. At high periplasmic ion concentrations, the arginine can be pushed off the site by the coupling ion, causing dissociation between rotor and stator. The rotor has now freedom for rotation within a small angle, which may be sufficient to move the site with the newly bound ion into an area, where an exchange with ions in the cytoplasmic reservoir becomes feasible (not the cytoplasmic channel). After rotating backwards, the ion is striped off from the site and diffuses into the periplasmic channel, while the

complex with the arginine reforms. Such an idling motion of the rotor versus the stator will lead to ion exchange between the two sides of the membrane, as observed experimentally for the Na^+ ATP synthase [59, 60].

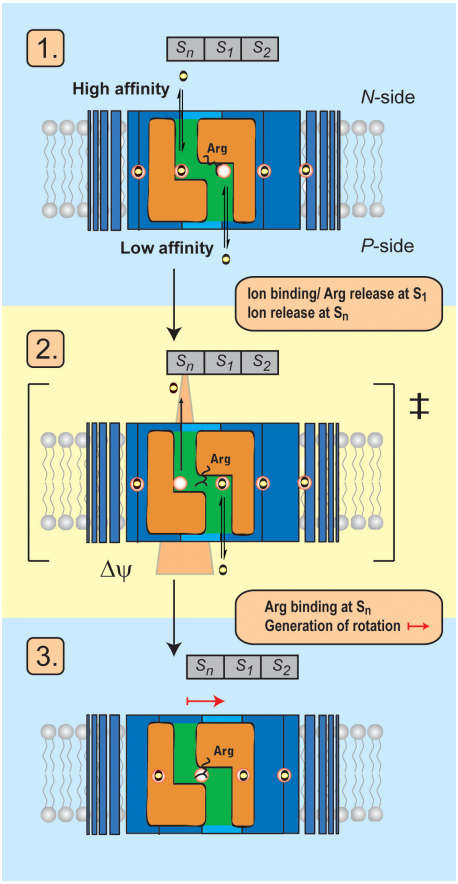

Figure 6. Events in the rotor/stator interface during ATP synthesis (rotation from left to right). Side view of the a/c interface of an F_0 motor. Shown is the c-ring (blue) with binding sites (red circles, S_1 to S_n) and subunit a containing the stator charge (Arg) and the (aqueous) P-side and the N-side access channels (green). In the starting position, the stator arginine is tightly bound to binding site S_1 **(1)**. Governed by chemical equilibria, which are influenced by the driving forces $\Delta\psi$ and $\Delta pH/\Delta pNa$, an incoming ion from the P-side is bound to site S_1 (requiring a high ion concentration), which displaces the Arg from the S_1 site. Simultaneously, the equilibria have to allow a release of an ion from the S_n site to the N-side, leading to a transition state in which the Arg is located between sites S_1 and S_n and the rotor is disconnected from the stator **(2)**. This allows the neutralized S_1 site to move into the lipid bilayer and the formation of an Arg-S_n complex in the interface, which generates unidirectional torque **(3)**. Browian motions are thought to bring the F_0 motor further into a new starting position (3. → 1.). See text for further details.

In the presence of appropriate driving forces, however, the motor will switch to unidirectional rotation and generate torque (Figure 6). In order to do so, the ion from the next incoming site must dissociate and escape through the cytoplasmic channel. This event is supported by a low ion concentration in the cytoplasmic reservoir, the positively charged arginine, and by the membrane potential. Attraction of the thus generated negatively charged, empty site by the positive stator charge causes rotation and generates torque. During the rotation step, the previously occupied site at the periplasmic channel is pushed out of the interface with subunit a and a new occupied site is pulled into the subunit a interface from the opposite side to contact the cytoplasmic access channel. The core feature of the new model is the so far unrecognized requirement for high coupling ion concentrations at the periplasmic side of the membrane. In the absence of these conditions, the motor is not functional, regardless of the magnitude of the applied driving forces. These new insights together with other observations suggest a torque generating mechanism, in which the electrostatic attraction of a negatively charged empty site by the positively charged arginine acts as the power stroke and where the driving forces serve to generate these positive and negative charges at the periplasmic and cytoplasmic channel, respectively.

Concluding Remarks

Finally, it should be emphasized that the F_o motor is highly asymmetric and appears to be perfectly constructed for $\Delta\mu H^+/\Delta\mu Na^+$-driven rotation in ATP synthesis direction. At sufficiently high periplasmic ion concentrations, the motor switches from its resting state with the arginine/binding site complex into a mobile state, where the binding site at the periplasmic channel has been occupied and the arginine has been liberated. This state provides a favourable provision for proceeding into ATP synthesis directed rotation, if the proper driving forces are applied. The only other option for the mobile state is to switch backwards into the resting state, if the periplasmic ion concentrations are reduced. For rotation into the opposite direction, it would be necessary to replace the arginine/binding site complex forming the resting state by ions from the cytoplasmic side of the membrane. Such a reaction can be excluded, however, at least for the Na^+ ATP synthase, since the rotation of the F_o motor in ATP hydrolysis direction was not driven by ΔpNa^+ [54, 59]. To prevent such unproductive movements into the wrong direction certainly increases the efficiency of the ATP synthase and may help to protect its structural integrity.

References

[1] Dimroth, P. (1997) Primary sodium ion translocating enzymes. *Biochim. Biophys. Acta* **1318**:11 – 51.
doi: 10.1016/S0005-2728(96)00127-2.

[2] Boyer, P.D. (1997) The ATP synthase – a splendid molecular machine. *Ann. Rev. Biochem.* **66**:717 – 749.
doi: 10.1146/annurev.biochem.66.1.717

[3] Capaldi, R.A., Aggeler, R. (2002) Mechanism of the F_1F_o-type ATP synthase, a biological rotaty motor. *Trends Biochem. Sci*. **27**:154 – 160.
doi: 10.1016/S0968-0004(01)02051-5.

[4] von Ballmoos, C., Cook, G.M., Dimroth, P. (2008) Unique rotary ATP synthase and its biological diversity. *Ann. Rev. Biophys*. **37**:43 – 64.
doi: 10.1146/annurev.biophys.37.032807.130018.

[5] von Ballmoos, C., Wiedenmann, A., Dimroth, P. (2009) Essentials for ATP synthesis by F_1F_o ATP synthases. *Ann. Rev. Biochem*. **78**:649 – 672.
doi: 10.1146/annurev.biochem.78.081307.104803.

[6] Abrahams, J.P., Leslie, A.G., Lutter, R., Walker, J.E. (1994) Structure at 2.8 Å resolution of F_1 ATPase from bovine heart mitochondria. *Nature* **370**:621 – 628.
doi: 10.1038/370621a0.

[7] Boyer, P.D. (1993) The binding change mechanism for ATP synthase – some probabilities and possibilities. *Biochim. Biophys. Acta* **1140**:215 – 250.
doi: 10.1016/0005-2728(93)90063-L.

[8] Noji, H., Yasuda, R., Yoshida, M., Kinosita Jr., K. (1997) Direct observation of the rotation of F_1-ATPase. *Nature* **386**:299 – 302.
doi: 10.1038/386299a0.

[9] Yasuda, R., Noji, H., Yoshida, M., Kinosita Jr., K., Itoh, H. (2001) Resolution of distinct rotational substeps by submillisecond kinetic analysis of F_1-ATPase. *Nature* **410**:898 – 904.
doi: 10.1038/35073513.

[10] Adachi, K., Oiwa, K., Nishizaka, T., Furuike, S., Noji, H., Itoh, H., Yoshida, M., Kinosita Jr., K. (2007) Coupling of rotation and catalysis in F_1-ATPase revealed by single-molecule imaging and manipulation. *Cell* **130**:309 – 321.
doi: 10.1016/j.cell.2007.05.020.

[11] Kaim, G., Prummer, M., Sick, B., Zumofen, G., Renn, A., Wild, U.P., Dimroth. P. (2002) Coupled rotation within single F_oF_1 enzyme complexes during ATP synthesis and hydrolysis. *FEBS Lett*. **525**:156 – 163.
doi: 10.1016/S0014-5793(02)03097-1.

[12] Diez, M., Zimmermann, B., Börsch, M., König, M., Schweinberger, E., Steigmiller, S., Reuter, R., Felekyan, S., Kudryavtsev, V., Seidel, C.A., Gräber, P. (2004) Proton-powered subunit rotation in single membrane-bound F_oF_1 ATP synthase. *Nat. Struct. Mol. Biol*. **11**:135 – 141.
doi: 10.1038/nsmb718.

[13] Düser, M.G., Zarrabi, N., Cipriano, D.J., Ernst, S., Glick, G.D., Dunn, S.D., Börsch, M. (2009) 36^o step size of proton-driven c-ring rotation in F_oF_1-ATP synthase. *EMBO J*. **28**:2689 – 2696.
doi: 10.1038/emboj.2009.213.

[14] Stock, D., Leslie, A.G., Walker, J.E. (1999) Molecular architecture of the rotary motor in ATP synthase. *Science* **286**:1700 – 1705.
doi: 10.1126/science.286.5445.1700.

[15] Pogoryelov, D., Nikolaev, Y., Schlatter, U., Pervushin, K., Dimroth, P., Meier, T. (2008) Probing the rotor subunit interface of the ATP synthase from *Ilyobacter tartaricus*. *FEBS J*. **275**:4850 – 4862.
doi: 10.1111/j.1742-4658.2008.06623.x.

[16] Valiyaveetil, F.I., Fillingame, R.H. (1998) Transmembrane topography of subunit a in the *Escherichia coli* F_1F_o ATP synthase. *J. Biol. Chem*. **273**:16241 – 16247.
doi: 10.1074/jbc.273.26.16241.

[17] Vik, S.B., Ishmukhametov, R.R. (2005) Structure and function of subunit a of the ATP synthase of *Escherichia coli*. *J. Bioenerg. Biomembr*. **37**:445 – 449.
doi: 10.1007/s10863-005-9488-6.

[18] Dunn, S., Revington, M., Cipriano, D., Shilton, B. (2000) The b subunit of *Escherichia coli* ATP synthase. *J. Bioenerg. Biomembr*. **32**:347 – 355.
doi: 10.1023/A:1005571818730.

[19] Greie, J.C., Deckers-Hebestreit, G., Altendorf, K. (2000) Subunit organization of the stator part of the F_o complex from *Escherichia coli* ATP synthase. *J. Bioenerg. Biomembr*. **32**:357 – 364.
doi: 10.1023/A:1005523902800.

[20] Weber, J. (2007) ATP synthase – the structure of the stator stalk. *Trends Biochem. Sci*. **32**:53 – 56.
doi: 10.1016/j.tibs.2006.12.006.

[21] Dickson, V.K., Silvester, J.A., Fearnley, I.M., Leslie, A.G., Walker, J.E. (2006) On the structure of the stator of the mitochondrial ATP synthase. *EMBO J*. **25**:2911 – 2918.
doi: 10.1038/sj.emboj.7601177.

[22] Meier, T., Polzer, P., Diederichs, K., Welte, W., Dimroth, P. (2005) Structure of the rotor ring of F-type Na^+-ATPase from *Ilyobacter tartaricus*. *Science* **308**: 659 – 662. doi: 10.1126/science.1111199.

[23] Oberfeld, B., Brunner, J., Dimroth, P. (2006) Phospholipids occupy the internal lumen of the c ring of the ATP synthase of *Escherichia coli*. *Biochemistry* **45**:1841 – 1851. doi: 10.1021/bi052304+.

[24] Vonck, J., Krug von Nidda, T., Meier, T., Matthey, U., Mills, D.J., Kühlbrandt, W., Dimroth, P. (2002) Molecular architecture of the undecameric rotor of a bacterial Na^+-ATP synthase. *J. Mol. Biol*. **321**:307 – 316. doi: 10.1016/S0022-2836(02)00597-1.

[25] von Ballmoos, C., Appoldt, Y., Brunner, J., Granier, T., Vasella, A., Dimroth, P. (2002) Membrane topography of the coupling ion binding site in Na^+-translocating F_1F_o ATP synthase. *J. Biol. Chem*. **277**:3504 – 3510. doi: 10.1074/jbc.M110301200.

[26] Meier, T., Krah, A., Bond, P.J., Pogoryelov, D., Diederichs, K., Fernaldo-Gomez, J.D. (2009) Complete coordination structure in the rotor ring of Na^+-dependent F-ATP synthase. *J. Mol. Biol*. **391**:498 – 507. doi: 10.1016/j.jmb.2009.05.082.

[27] Murata, T., Yamato, I., Kakinuma, Y., Leslie, A.G., Walker, J.E. (2005) Structure of the rotor of the V-type Na^+-ATPase from *Enterococcus hirae*. *Science* **308**:654 – 659. doi: 10.1126/science.1110064.

[28] Pogoryelov, D., Yildiz, O., Fernaldo-Gomez, J.D., Meier, T. (2009) High-resolution structure of the rotor ring of a proton-dependent F-ATP synthase. *Nat. Struct. Mol. Biol*. **16**:1068 – 1073. doi: 10.1038/nsmb.1678.

[29] Preiss, L., Yldiz, O., Hicks, D.B., Krulwich, T.A., Meier, T. (2010) A new type of proton coordination in an F_1F_o-ATP synthase rotor ring. *PLoS Biology* **8**:1 – 10. doi: 10.1371/journal.pbio.1000443.

[30] Dautant, A., Velours, J., Giraud, M.F. (2010) Crystal structure of the Mg.ADP-inhibited state of the yeast F_1c_{10} ATP synthase. *J. Biol. Chem*. **285**(38):29502 – 29510. doi: 10.1074/jbc.M110.124529.

[31] von Ballmoos, C., Dimroth, P. (2007) Two distinct proton binding sites in the ATP synthase family. *Biochemistry* **46**:11800 – 11809. doi: 10.1021/bi701083v.

[32] Krah, A., Pogoryelov, D., Langer, J., Bond, P.J., Meier, T., Feraldo-Gomez, J.D. (2010) Structural and energetic basis for H^+ versus Na^+ binding selectivity in ATP synthase F_o rotors. *Biochim. Biophys. Acta* **1797**:763 – 772.
doi: 10.1016/j.bbabio.2010.04.014.

[33] Meier, T., Matthey, U., von Ballmoos, C., Vonck, J., Krug von Nidda, T., Kühlbrandt, W., Dimroth, P. (2003) Evidence for structural integrity in the undecameric c-rings isolated from sodium ATP synthases. *J. Mol. Biol*. **325**:389 – 397.
doi: 10.1016/S0022-2836(02)01204-4.

[34] von Ballmoos, C., Meier, T., Dimroth, P. (2002) Membrane-embedded location of Na^+ or H^+ binding sites on the rotor ring of F_1F_o ATP synthases. *Eur. J. Biochem*. **269**:5581 – 5589.
doi: 10.1046/j.1432-1033.2002.03264.x.

[35] Junge, W., Lill, H., Engelbrecht, S. (1997) ATP synthase: an electrochemical transducer with rotary mechanics. *Trends Biochem. Sci*. **22**:420 – 423.
doi: 10.1016/S0968-0004(97)01129-8.

[36] Angevine, C.M., Herold, K.A., Fillingame, R.H. (2003) Aqueous access pathways in subunit a of rotary ATP synthase extend to both sides of the membrane. *Proc. Natl. Acad. Sci. U.S.A.* **100**:131779 – 13183.
doi: 10.1073/pnas.2234364100.

[37] Angevine, C.M., Fillingame, R.H. (2003) Aqueous access channels in subunit a of rotary ATP synthase. *J. Biol. Chem*. **278**:6066 – 6074.
doi: 10.1074/jbc.M210199200.

[38] Steed, P.R., Fillingame, R.H. (2009) Aqueous accessibility of the transmembrane regions of subunit c of the *Escherichia coli* F_1F_o ATP synthase. *J. Biol. Chem*. **284**:23243 – 23250.
doi: 10.1074/jbc.M109.002501.

[39] Jiang, W., Fillingame, R.H. (1998) Interacting helical faces of subunits a and c in the F_1F_o ATP synthase of *Escherichia coli* defined by disulfide cross-linking. *Proc. Natl. Acad. Sci. U.S.A.* **95**:6607 – 6612.
doi: 10.1073/pnas.95.12.6607.

[40] Vorburger, T., Zingg Ebneter, J., Wiedenmann, A., Morger, D., Weber, G., Diederichs, K., Dimroth, P., von Ballmoos, C. (2008) Arginine-induced conformational change in the c-ring/a-subunit interface of the ATP synthase. *FEBS J*. **275**:2137 – 2150.
doi: 10.1111/j.1742-4658.2008.06368.x.

[41] Lau, W.C.Y., Rubinstein, J.L. (2010) Structure of intact *Thermus thermophilus* V-ATPase by cryo-EM reveals organization of the membrane-bound V_o motor. *Proc. Natl. Acad. Sci. U.S.A.* **107**:1367 – 1372. doi: 10.1073/pnas.0911085107.

[42] Cain, B.D., Simoni, R.D. (1989) Proton translocation by the F_1F_o ATPase of *Escherichia coli*. Mutagenic analysis of the a subunit. *J. Biol. Chem*. **264:**3292 – 3300.

[43] Wehrle, F., Kaim, G., Dimroth, P. (2002) Molecular mecuanism of the ATP synthase's F_o motor probed by mutational analyses of subunit a. *J. Mol. Biol*. **322**:369 – 381. doi: 10.1016/S0022-2836(02)00731-3.

[44] Xing, J., Wang, H., von Ballmoos, C., Dimroth, P., Oster, G. (2004) Torque generation by the F_o motor of the sodium ATPase. *Biophys. J.* **87**:2148 – 2163. doi: 10.1529/biophysj.104.042093.

[45] Mitchell, P. (1961) Coupling of phosphorylation to electron and hydrogen transfer by a chemi-osmotic type of mechanism. *Nature* **191**:144 – 148. doi: 10.1038/191144a0.

[46] Jagendorf, A.T., Uribe, E. (1966) ATP formation caused by acid-base transition of spinach chloroplasts. *Proc. Natl. Acad. Sci. U.S.A.* **55**:170 – 177. doi: 10.1073/pnas.55.1.170.

[47] Kaim, G., Dimroth, P. (1999) ATP synthesis by F-type ATP synthase is obligatorily dependent on the transmembrane voltage. *EMBO J.* **18**:4118 – 4127. doi: 10.1093/emboj/18.15.4118.

[48] Mitchell, P. (1966) Chemiosmotic coupling in oxidative and photosynthetic phosphorylation. *Biol. Rev. Cam. Philos. Soc*. **41**:445 – 502. doi: 10.1111/j.1469-185X.1966.tb01501.x.

[49] Cockrell, R.S., Harris, E.J., Pressman, B.C. (1967) Synthesis of ATP driven by a potassium gradient in mitochondria. *Nature* **215**:1487 – 1488. doi: 10.1038/2151487a0.

[50] Maloney, P.C., Wilson, T.H. (1975) ATP synthesis driven by a proton motive force in *Streptococcus lactis*. *J. Membr. Biol*. **25**:285 – 310. doi: 10.1007/BF01868580.

[51] Sone, N., Yoshida, M., Hirata, H., Kagawa, Y. (1977) Adenosine triphosphate synthesis by electrochemical proton gradient in vesicles reconstituted from purified adenosine triphosphatase and phospholipids from thermophilic bacterium. *J. Biol. Chem*. **252**:2956 – 2960.

[52] Fischer, S., Gräber, P. (1999) Comparison of ΔpH-and Δψ-driven ATP synthesis catalyzed by the ATPase from *Escherichia coli* or chloroplasts reconstituted into liposomes. *FEBS Lett*. **457**:327 – 332.
doi: 10.1016/S0014-5793(99)01060-1.

[53] Etzold, C., Deckers-Hebestreit, G., Altendorf, K. (1997) Turnover number of *Escherichia coli* F_oF_1 ATP synthase in membrane vesicles. *Eur. J. Biochem.* **243**:336 – 343.
doi: 10.1111/j.1432-1033.1997.0336a.x.

[54] Wiedenmann, A., Dimroth, P., von Ballmoos, C. (2009) Functional asymmetry of the F_o motor in bacterial ATP synthases. *Mol. Microbiol*. **72**:479 – 490.
doi: 10.1111/j.1365-2958.2009.06658.x.

[55] Williams, R.J. (1978) The multifarious coupling of energy transduction. *Biochim. Biophys. Acta* **505**:1 – 44.

[56] Laubinger, W., Dimroth, P. (1988) Characterization of the ATP synthase of *Propionigenium modestum* as a primary sodium pump. *Biochemistry* **27**:7531 – 7537.
doi: 10.1021/bi00419a053.

[57] Kluge, C., Dimroth, P. (1993) Kinetics of inactivation of the F_1F_o ATPase of *Propionigenium modestum* by dicyclohexylcarbodiimide in relationship to H^+ and Na^+ coordination: probing the binding site for thje coupling ions. *Biochemistry* **32**:10378 – 10386.
doi: 10.1021/bi00090a013.

[58] Wiedenmann, A., Dimroth, P., von Ballmoos, C. (2008) Δψ and ΔpH are equivalent driving forces for proton transport through isolated F_o complexes of ATP synthases. *Biochim. Biophys. Acta* **1777**:1301 – 1310.
doi: 10.1016/j.bbabio.2008.06.008.

[59] Kluge, C., Dimroth, P. (1992) Studies on Na^+ and H^+ translocation through the F_o part of the Na^+-translocating F_1F_o ATPase from *Propionigenium modestum*: discovery of a membrane potential dependent step. *Biochemistry* **31**:12665 – 12672.
doi: 10.1021/bi00165a017.

[60] Kaim, G., Dimroth, P. (1998) Voltage-generated torque drives the motor of the ATP synthase. *EMBO J*. **17**:5887 – 5895.
doi: 10.1093/emboj/17.20.5887.